AIP Conference Proceedings

RESEARCH ARTICLE | OCTOBER 06 2023

A numerical radiation model for the centrifugal particle solar receiver FREE

Serdar Hicdurmaz; Johannes Grobbel; Reiner Buck; Bernhard Hoffschmidt

Check for updates

AIP Conf. Proc. 2815, 100005 (2023)
https://doi.org/10.1063/5.0148791

View Online
Export Citation
CrossMark

20 November 2023 12:58:51

AIP Publishing

A Numerical Radiation Model for the Centrifugal Particle Solar Receiver

Serdar Hicdurmaz [1, a)], Johannes Grobbel [2], Reiner Buck [1], Bernhard Hoffschmidt [3]

[1]German Aerospace Center (DLR), Institute of Solar Research 70569 Stuttgart, Germany
[2]German Aerospace Center (DLR), Institute of Future Fuels 52428 Juelich, Germany
[3]German Aerospace Center (DLR), Institute of Solar Research 51147 Cologne, Germany.

[a)] Corresponding author: serdar.hicdurmaz@dlr.de

Abstract. The centrifugal particle solar receiver (CentRec) is a promising technology to reduce the cost of heat and electricity generated by solar towers. In this study, a computationally inexpensive radiation model accounting for all radiative heat transfer mechanisms in the CentRec is addressed. A short-range radiation model to calculate the radiative heat transfer between close particle pairs and a radiation enclosure model to calculate diffuse radiation heat exchange between large surfaces of the receiver are developed. Moreover, a radiation penetration model to distribute the solar energy to particles, which was developed by authors previously, is integrated into the main model. The models are applied to a small-scale receiver and thermal steady state results are obtained. The model is compared with an in-house Monte Carlo ray tracing code for the case of a uniform heat flux of 3 MW/m^2 at the aperture. The results show that although the developed model matches particle outlet temperature by a narrow margin (10 K), the temperature distribution in the receiver is overestimated slightly by the current model. Moreover, while the current model calculates around 3.5% of reflection and emission loss, MCRT-based model gives around 5.5% of total radiative loss for the given solar flux distribution. Thus, there is still room for improvement.

20 November 2023 12:58:51

INTRODUCTION

Particle solar receivers promise higher thermal efficiency and lower operational and component cost compared to the molten salt-based solar receivers in solar tower applications [1]. The centrifugal particle solar receiver (CentRec) is a direct absorption receiver concept where the ceramic particles descend through the inclined rotating drum while being exposed to solar beams concentrated by a heliostat field. Thanks to the gravity and centrifugal effects, an optically opaque but sufficiently thin particle film can be obtained on the receiver inner wall, as shown in Fig. 1a. During the movement of particles as a bulk, photons intersecting the aperture plane strike the moving particle film and directly heat up the particles. Depending on the receiver rotation speed and the particle mass flow rate, one can adjust the particle outlet temperature for various flux conditions. The CentRec has been demonstrated to reach 965°C of particle outlet temperature at the Juelich Solar Tower [2].

Optimization of the particle motion to enhance the receiver thermal efficiency is crucial. A set of experiments for various receiver rotation speeds and particle mass flow rates was conducted by the authors in a previous study to understand the flow characteristics of the particle film [3]. Also, a Discrete Element Method (DEM) based numerical model was developed and particle properties such as the particle friction coefficients were calibrated. An open source DEM tool, LIGGGHTS, is employed to model the particle motion (Fig. 1b). Finally, a heat transfer model accounting for particle scale conduction and short-range radiation, receiver scale long-range radiation and convection models was developed by the authors [4, 5]. The radiation heat transfer is the main heat transfer mechanism in the CentRec because the particles are heated up by the solar radiation while they lose energy by radiation, convection and conduction [4]. A common approach to numerically model the radiation in such particle receivers is ray tracing [4-6]. However, ray tracing-based radiation models lead to high computational burden compared to other heat transfer mechanisms such

SolarPACES: Solar Power & Chemical Energy Systems
AIP Conf. Proc. 2815, 100005-1–100005-9; https://doi.org/10.1063/5.0148791
Published by AIP Publishing. 978-0-7354-4623-6/$30.00

as particle scale conduction. In order to overcome this problem, a computationally cheaper model considering the short-range radiation, long-range radiation and solar beam penetration models are separately addressed in this study.

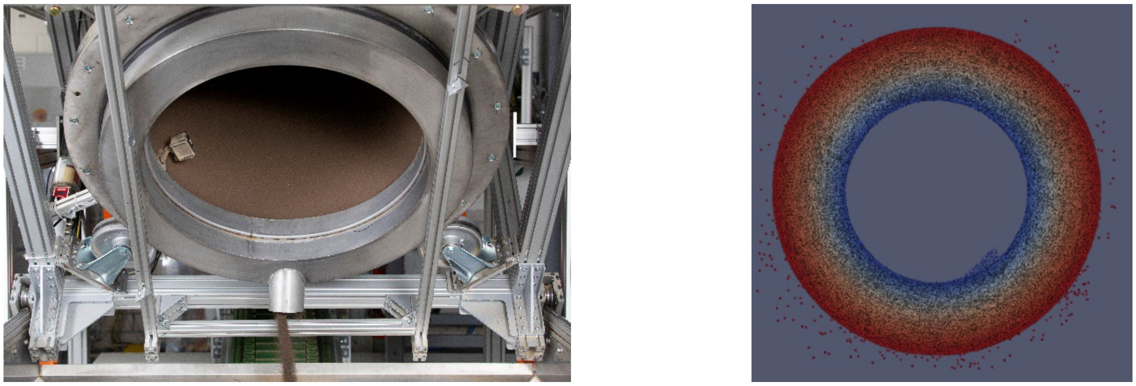

(a) (b)

FIGURE 1. (a) Experiment-scale receiver with moving particles (b) A snapshot from the DEM particle simulation.

NUMERICAL MODEL

In the CentRec simulation, the particle dynamics model and heat transfer calculations are separated from each other by assuming the DEM collision and contact properties are temperature-independent. By doing so, it is avoided to re-run computationally costly DEM simulations whenever a different flux condition is applied to the same particle configuration. First, the position of the particles in the simulation, generated by LIGGGHTS in each thermal coupling time step, are stored. Then, a thermal code developed in MATLAB is applied to the particles to find the temperature distribution inside the receiver. In this study, only the radiation mode of the heat transfer is considered while other heat transfer modes are switched off. Three different sub-models comprising the complete radiation model are listed below.

- The solar beam radiation striking the particle film and the reflections from the particle surface.
- The short-range radiation occurring between close particle pairs and between particle - wall pairs.
- The long-range radiation occurring between the large surfaces within the receiver, including cold and hot regions of the particle film, the inlet distributor, the collector ring and the aperture.

20 November 2023 12:58:51

Beam Radiation Penetration Model

In the CentRec, rays strike the moving particle film at incidence angles mostly between 15° and 65° [7]. The incidence angle is defined as the angle between the rotation axis of the receiver and the vector representing the incoming ray in space such that it varies between 0° and 90°. The authors have shown in the previous study that the radiation penetration behavior in a particle bed can be characterized as a function of bed bulk solid fraction, incidence angle and particle emissivity if gray and diffuse particles are assumed [7]. In Fig. 2, the transmitted fraction of rays as a function of bed depth is plotted for a representative solid fraction, particle emissivity and various incidence angles. It can be noticed that the transmission decay is non-linear in the first 0-2 radii region whereas a linear decay occurs after 2 radii. These two regions can be characterized by an exponential and a linear fit for any incidence angle, bulk solid fraction and particle emissivity triplet. Moreover, one can also estimate the bulk reflectivity, which is also a function of this triplet. The bulk reflectivity and transmission equation formulas are given in [7]. The procedure to distribute the energy of the rays to the particles is mainly as follows:

- The bulk solid fraction of the particle domain is estimated.
- The bulk reflectivity and absorptivity are found by using the incidence angle, particle emissivity and bulk solid fraction.
- By using transmission equations, the absorbed energy by the bulk is distributed to the particles based on their distance to the film surface. The details of the heat distribution algorithm can be found in [7].

In Fig. 3, the transmission behavior of the bed found by the current approach is compared with the results of an open source Monte Carlo ray tracing code for two different CentRec cases [7, 8]. First, it should be noted that the local solid fraction (black solid line) is oscillating due to the presence of the wall. A bulk solid fraction (black dashed line), which is the value that the bed converges to if the film thickness would be thick enough, can be estimated by using the peaks and dips of the oscillation [7]. The results for 15° - 60° incidence angle show that the current model estimates the transmission decay very well for both cases. It should be noted that the shape of the transmission curve highly depends on local solid fraction distribution, as can be seen in Fig. 3.

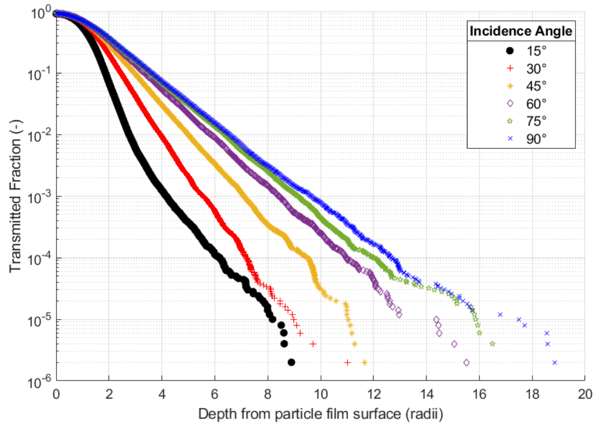

FIGURE 2. Transmission behavior of bed with 0.5 of SF for various incidence angle. Particle emissivity is 0.86.

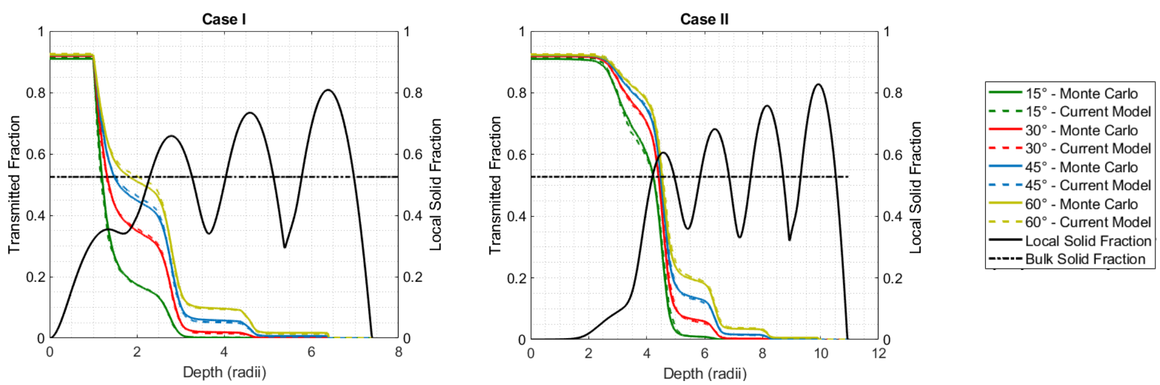

(a) (b)

FIGURE 3. Comparison of transmitted fraction decays found by Monte Carlo ray tracing and the current model as a function of absorption depth for two different CentRec cases. Particle emissivity is 0.86. The “0” depth corresponds the topmost particle radial position plus 1 particle radius.

20 November 2023 12:58:51

Short-Range Radiation Model

In this study, particle-particle and particle-wall radiation distribution factors are used to calculate the short-range radiation, which occurs between a particle, its nearby particles and the wall. The Radiation Distribution Factor (RDF) is the proportion of rays emitted from particle A and reaching particle B not only directly but also via reflections from other surrounding particles. Johnson et al. [9] derived distance based RDF’s for various particle emissivities and uniform bulk solid fractions. However, in the CentRec application, the local solid fraction is oscillating due to the proximity of the particles to the wall. Thus, a new correlation is derived which is applicable to the CentRec application by using the open source Monte Carlo code [9]. In Fig. 4a, particle – particle RDFs (blue dots) are plotted against the particle – particle distance. The particles touching the wall are not considered here because for a non-black wall case, they absorb a very high portion of the reflections from the wall. Moreover, because they are stationary relative to the rotating receiver during operation thanks to a wire mesh welded on the cylindrical receiver wall, their temperature is almost the same as the local wall temperature during operation [10]. As can be seen in Fig. 4a, a curve fit (red line) is found by averaging MCRT results. The results show that the precision of the curve fit is decreasing especially after

3 radii. In Fig. 4b, by using the same approach, the particle-wall RDF is derived. In order to check the validity of the found curve fit, a $30d_p$ x $30d_p$ x 8 d_p domain is considered, where d_p is the particle diameter. The temperature of a wall and particles touching the wall is set to 1000 K, while the one of particles being more distant to the wall than $5d_p$ are set to 1100K. Then, the heat transfer along z-direction is calculated between two constant temperature zones by using the actual RDFs found by the MCRT code and RDF curve fit. The z-direction is defined as the direction normal to the wall such that wall presents at z=0. The difference in heat transfer is found to be less than 3%. Thus, it is assumed the current approach is valid.

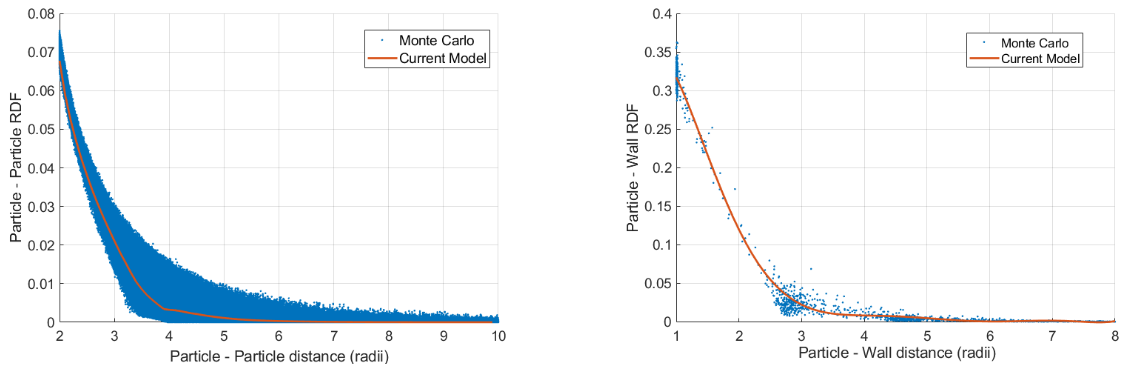

(a) (b)

FIGURE 4 Distance-based RDF curves fitted by using Monte Carlo ray tracing results. (a) Particle–particle RDFs as a function of particle–particle center distance (b) Particle – wall RDFs as a function of particle center–wall distance. Particle emissivity is 0.86 and wall emissivity is 0.4.

20 November 2023 12:58:51

Radiation Enclosure Model

In the CentRec, radiation heat exchange does not only occur between close particle pairs but also among the large surfaces within the receiver, including cold and hot regions of the particle film, the particle distributor, the collector ring and the aperture, as can be seen in Fig. 5b. All these surfaces form a radiation enclosure in which diffuse radiation heat exchange occurs between all surface pairs based on surface emissivity and temperature. The solar radiation carried by photons also circulates in the cavity as reflected radiation until it is eventually absorbed by any surface. In order to build a radiation enclosure model, all surfaces are assumed as gray and diffuse. First, the particle film surface is meshed with rectangular type elements as shown in Fig. 5a. Later, the top plate (particle distributor), bottom ring (collector ring) and aperture plane is defined in the radiation model. Actually, these surfaces do not exist in the DEM model for the sake of model simplicity but they are employed in the real application. The surfaces are shown in Fig. 5b. By means of the geometrical configuration of all surfaces, one can calculate the view factor between each surface pair analytically. In this study, analytical expressions from literature are employed [11].

In order to find the radiative heat transfer to/from each element, a derivation for radiosity and irradiation for an element should be made. First, an energy balance can be written for a surface as

$$q^{||} = J - G^d - G^s \tag{1}$$

$$J = E + \rho^d G^d + \rho^s G^s \tag{2}$$

$q^{||}$, J, G and E are the net heat flux to the surface, the radiosity, the irradiation and the emission, respectively. ρ is the reflectivity, where superscripts "s" and "d" stand for specular and diffuse. The radiosity from a surface is simply the summation of emission and reflected specular and diffuse irradiation as stated in Equation 2. For a gray and diffuse surface, emissivity (ε) is same as the absorptivity (α) and equals to $(1-\rho)$. Thus, Equation 2 can be rewritten as

$$J = \varepsilon^d E_b + (1-\varepsilon^d)\cdot G^d + (1-\varepsilon^s)\cdot G^s \tag{3}$$

The diffuse irradiation can be defined by using Equation 3.

$$G^d = \frac{J - \varepsilon^d E_b - (1 - \varepsilon^s) \cdot G^s}{(1 - \varepsilon^d)} \tag{4}$$

If Equation 4 is inserted into Equation 1 and reorganized, one can obtain

$$q^{||} = \frac{\varepsilon^d (E_b - J) + (\varepsilon^d - \varepsilon^s) \cdot G^s}{(1 - \varepsilon^d)} \tag{5}$$

Diffuse irradiation to surface *i* can also be written in the following form

$$A_i G_i^d = \sum_{j=1}^{n} F_{ji} A_j J_j \tag{6}$$

A and F_{ji} is the surface area and view factor from surface *j* to *i*. From the reciprocity rule, one can write

$$F_{ji} A_j = F_{ij} A_i \tag{7}$$

Thus, Equation 6 can be written as

$$G_i^d = \sum_{j=1}^{n} F_{ij} J_j \tag{8}$$

If Equation 8 is inserted into Equation 1, one can obtain

$$q_i^{||} = J_i - \sum_{j=1}^{n} F_{ij} J_j - G_i^s \tag{9}$$

Thus, the heat flux can be written in two forms as seen in Equation 5 and 9. One can equate both equations and leave the unknown radiosity terms on the left-hand side. For surface *i*, the general radiation equation is written as

$$\left((1 - \varepsilon^d) F_{ii} + \varepsilon^d\right) J_i - \sum_{\substack{j=1 \\ j \neq i}}^{n} (1 - \varepsilon^d) F_{ij} J_j = \varepsilon^d E_{b,i} + (1 - \varepsilon^s) G_i^s \tag{10}$$

One can write Equation 10 for each surface in the enclosure model. By doing so, one can construct coefficient matrix A and right-hand side vector B such that [A][J] = [B]. Then, this matrix system is solved and radiosity from/to each surface can be found. Finally, the net heat flux to a surface can be found by using Equation 5. Note that ε^d and ε^s are different for each particle surface mesh because they are a function of incidence angle and bulk solid fraction. In the CentRec application G_i^s is the solar irradiation to surface *i.*

MODEL APPLICATION

The complete radiation model described above is applied to a small sized CentRec to compare with the Monte Carlo ray tracing-based model. The model parameters are listed in Table 1. First, a DEM simulation is run for 120s to obtain the particle positions in each thermal time step. As can be seen in Fig. 6, the inlet and outlet mass flow rates are equal to each other after 30 seconds, thus one can say that the system reached cold steady-state. At 30 s, a uniform flux with constant incidence angle is applied at the aperture plane. The flux distribution on the receiver wall is shown in Fig. 7. In this model, a square mesh size of 10d_p is selected after a mesh refinement study, which yields 31 and 14 mesh elements in tangential and axial direction. Then, by using the flux distribution, an average power hitting each

20 November 2023 12:58:51

mesh element is found. Although the incidence angle is constant at the aperture plane, it is slightly different on the receiver wall due to the wall's cylindrical shape. Thus, a sine-averaged incidence angle is also calculated for each mesh element.

A Monte Carlo ray tracing code developed by the authors [5] is also run in parallel to validate the developed model. The details of the code are not mentioned here for brevity.

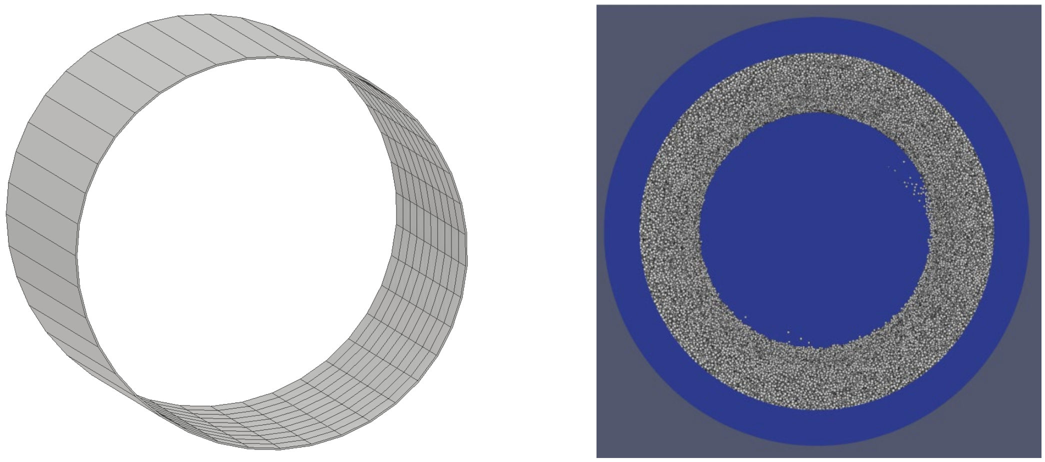

(a) (b)

FIGURE 5. (a) Meshed Receiver Surface. (b) CentRec simulation with extra surfaces considered in the radiation enclosure model. The back blue surface is a pseudo particle distributor and the front blue ring is a pseudo collector ring.

20 November 2023 12:58:51

TABLE 1. Input Parameters

Parameter	Unit	Value
Cavity diameter	cm	12
Aperture diameter	cm	10
Cavity length	cm	17.1
Particle diameter	mm	1.2
Mass flow rate	kg/s	0.0357
Rotational speed	rpm	160
Initial temperature for all surfaces	K	673.15
Particle inlet temperature	K	673.15
Particle emissivity	-	0.86
Wall emissivity	-	0.4
Aperture plane temperature	K	0
Uniform flux at aperture	MW/m^2	3
Uniform incidence angle at aperture	°	45
Thermal time step	s	0.1

RESULTS

The radiation models can be best compared to the MCRT results when the system reaches thermal steady state. Because the cylindrical wall is the element reaching steady state latest, its temperature is monitored as the simulation progresses. As seen in Fig. 8a, the change in the wall temperature is very small after 90s. Thus, the results at 90s are assumed as steady state. First, particle outlet temperatures and receiver efficiencies are compared in Fig. 8b. Because radiation is the only heat transfer mode in this model, the heat loss is the summation of reflection loss and emission loss. In Fig. 8b, it is seen that there is 2% efficiency difference between the two models. While the MCRT based model predicts 1.4% and 2.3% of reflection and emission loss, respectively, the current model estimates 2.3% and 3.2%. It means that the current model overestimates MCRT based results slightly. Regarding the difference in reflection loss, the current model may give a slightly erroneous result due to the diffuse reflection assumption on the particle film surface. This assumption will be validated in a future study. Although there is a deviation in efficiency values, there is only about a 10 K temperature difference in particle outlet temperature between the two models. However, near the end of the receiver this difference diminishes to some extent.

In Fig. 8c, the temperatures of the particle layers with thickness 1 particle diameter are compared at steady state conditions. Although for the first two layers next to wall the temperature distribution is close to the one obtained by MCRT, there is around 50 K difference in the 3rd and 4th layers, especially at the axial position where the flux is at peak.

All in all, there are some discrepancies between MCRT and the current models although the thermal behavior is very similar. The computational burden of the current model scales significantly less with particle number than the MCRT model and hence can be considered to be numerically more feasible, in particular for larger receivers with many particles. Hence, there is motivation to further optimize and improve the current model, so that the deviations to the MCRT model become even smaller.

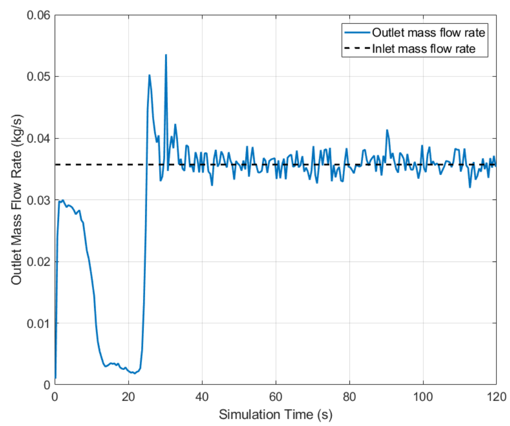

FIGURE 6. Particle outlet mass flow rate vs simulation time

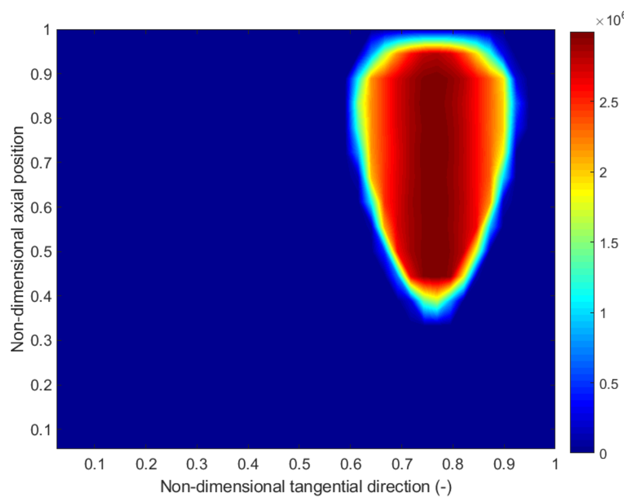

FIGURE 7. Flux distribution on the receiver wall. The unit of the contour is W/m^2

20 November 2023 12:58:51

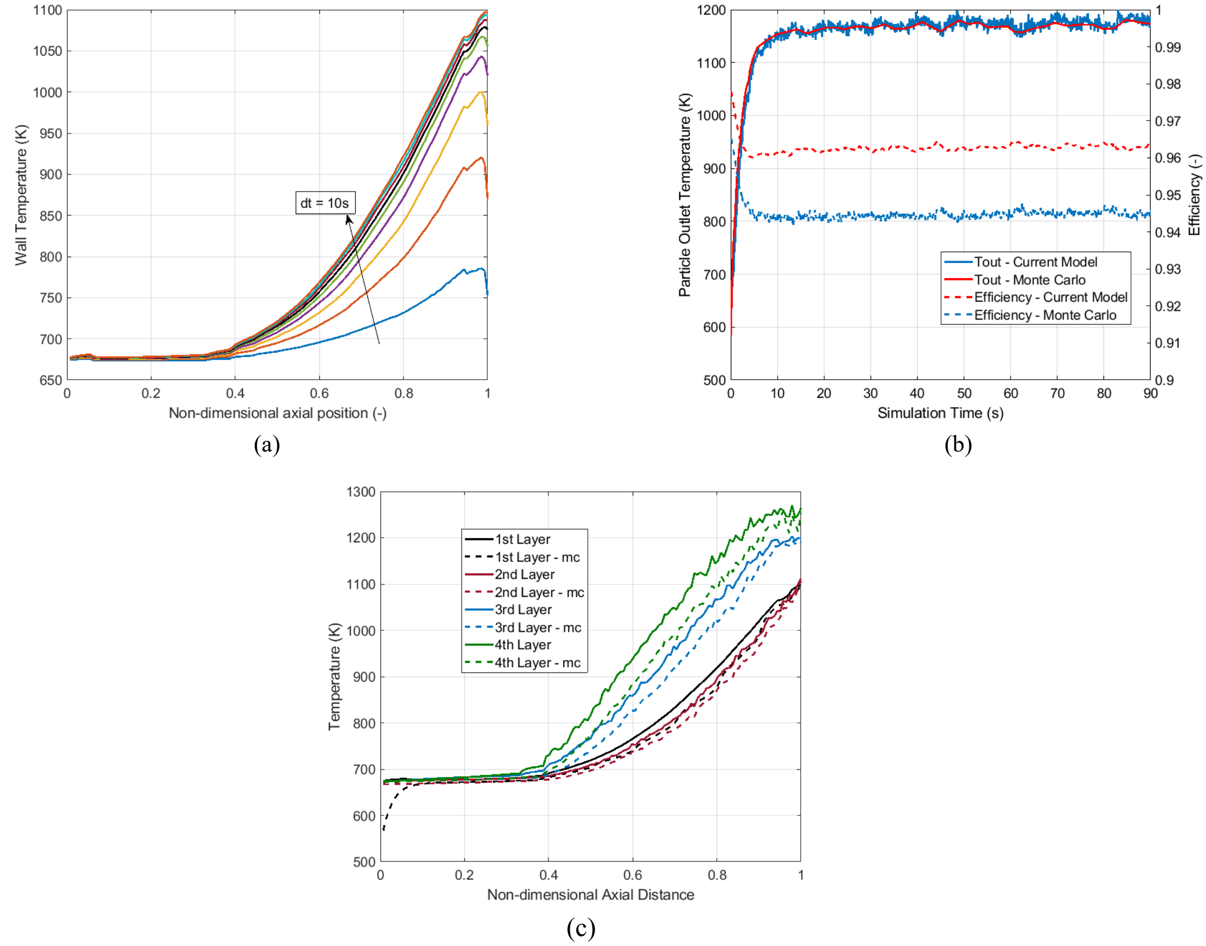

FIGURE 8. (a) Wall temperature distribution for different time steps found by current model (b) Particle outlet temperature and overall efficiency for each model (c) Temperature distribution in each particle layer at t=90 s.

CONCLUSION

In this study, a complete radiation model is addressed to reduce the computational burden resulting from computationally expensive ray tracing models. A short-range radiation model being available in literature is tailored for the CentRec application. Moreover, a radiation enclosure model accounting for reflections and emission within the cavity is developed. A radiation penetration model which was developed by authors previously is also employed to find radiation penetration behavior of incoming solar flux. The results have shown that although the current model estimates the temperature distribution to some extent, there is a slight but non-negligible error. Because the short-range radiation model and radiation penetration model are validated, the error is likely due to the radiation enclosure model. Thus, the authors will focus to minimize this error in their future work. The assumption that reflections and emissions from particle film surface are diffuse will be revised, and radiation enclosure model will be further validated.

ACKNOWLEDGMENTS

This work is supported by DLR – DAAD Research Fellowship Programme.

20 November 2023 12:58:51

REFERENCES

1. Ho C.K., *A review of high-temperature particle receivers for concentrating solar power.* Applied Thermal Engineering, 2016. **109**: p. 958-969.
2. Ebert M., Amsbeck L., Buck R., Rheinländer J., Schloegl-Knothe B., Schmitz S., Sibum M., Stadler H., Uhlig R., *First on-sun tests of a centrifugal particle receiver system*. Proceedings of the ASME 2018 Power and Energy Conference PowerEnergy 2018. Lake Buena Vista, Florida, USA.
3. Hicdurmaz, S., Buck R., Hoffschmidt B., *Image Analysis of Particle Flow in Centrifugal Solar Particle Receiver*. Journal of Solar Energy Engineering (accepted), 2021. 10.1115/1.4053464
4. Hicdurmaz, S., Johnson E.F., Grobbel J., Amsbeck L., Buck R., Hoffschmidt B., *Numerical Heat Transfer Modelling of a Centrifugal Solar Particle Receiver (accepted)*. SolarPACES 2020, AIP Conference Proceedings: Virtual Conference.
5. Grobbel, J., *Modeling Solar Particle Receivers with the Discrete Element Method*. PhD Thesis, RWTH Aachen University, 2019.
6. Johnson, E.F., *Advances in Modeling High Temperature Particle Flows in Concentrating Solar Power*. PhD Thesis, Middle East Technical University, 2021.
7. Johnson, E.F., Hicdurmaz, S., Buck R., Hoffschmidt B., *Beam Radiation Penetration in Particle Beds, for Heat Transfer Modeling in the Discrete Element Method.* Journal of Quantitative Spectroscopy and Radiative Transfer, 2021 (submitted).
8. Johnson, E., Tarı I., Baker D., *A Monte Carlo Method to Solve for Radiative Effective Thermal Conductivity for Particle Beds of Various Solid Fractions and Emissivities.* Journal of Quantitative Spectroscopy and Radiative Transfer, 2020. **250**. 10.1016/j.jqsrt.2020.107014
9. Johnson, E.F., Tarı I., Baker D., *Radiative heat transfer in the discrete element method using distance based approximations.* Powder Technology, 2021. **380**: p. 164–182.
10. Amsbeck, L., Buck R., Ebert M., Gobereit B., Hertel J., Jensch A., Rheinlander J., Trebing D., Uhlig R., *First Tests of a Centrifugal Particle Receiver with a 1m2 Aperture*. SolarPACES. 2017, AIP Conference Proceedings: Santiago, Chile.
11. Howell, J.R. *A Catalog of Radiation Heat Transfer Configuration Factors*. [cited 2021 September 28]; Available from: http://www.thermalradiation.net/tablecon.html.

20 November 2023 12:58:51